Science of the Total Environment 646 (2019) 1069–1079

Contents lists available at ScienceDirect

Science of the Total Environment

journal homepage: www.elsevier.com/locate/scitotenv

rDNA- and rRNA-derived communities present divergent assemblage patterns and functional traits throughout full-scale landfill leachate treatment process trains

Duntao Shu [a], Jianhua Guo [b], Baogang Zhang [a], Yanling He [c,*], Gehong Wei [a,*]

[a] State Key Laboratory of Crop Stress Biology in Arid Areas, College of Life Sciences, Northwest A&F University, Yangling, Shaanxi 712100, China
[b] Advanced Water Management Centre (AWMC), The University of Queensland, St Lucia, Brisbane, QLD 4072, Australia
[c] School of Human Settlements & Civil Engineering, Xi'an Jiaotong University, Shaanxi 710049, China

HIGHLIGHTS

- The relative contribution by rare taxa to total activity did not follow abundance.
- rDNA- and rRNA-based community present divergent assemblage patterns.
- Functional traits dominate the assembly of core and whole bacterial communities.
- Habitat filtering and niche differentiation drives expression of N-cycling genes.

GRAPHICAL ABSTRACT

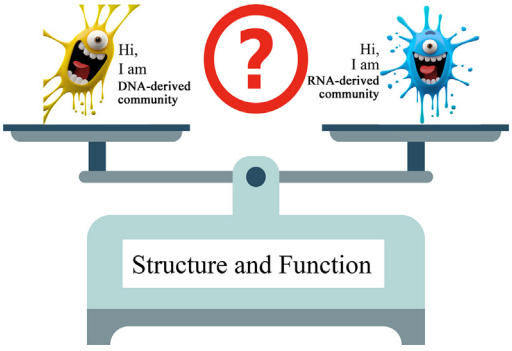

ARTICLE INFO

Article history:
Received 10 May 2018
Received in revised form 26 July 2018
Accepted 27 July 2018
Available online 29 July 2018

Editor: Zhen (Jason) He

Keywords:
Microbial community
Nitrogen cycling
Functional gene
Taxon-habitat association
rRNA

ABSTRACT

Understanding the influences of microbial interactions and niche heterogeneities on microbial communities and functional traits is critical for determining its engineering and ecological significance. However, little is known about microbial community assemblage and functional gene expression throughout full-scale landfill leachate treatment plants. Here, we applied a combination of 16S rRNA and rDNA amplicon sequencing, shotgun metagenomic, and qPCR approaches to unveil the ecological associations between distinct communities, functional gene expression and nitrogen cycling processes. By comparing the rDNA and rRNA-derived communities, the rRNA/rDNA ratios suggested that 57.2% of rare taxa were active, and their abundance decreased as increasing of potential activities. In particular, rDNA- and rRNA-based communities exhibited divergent assemblage patterns, and stronger intra-associations among core taxa in the rRNA-based communities than in rDNA-based communities. Furthermore, results regarding both bacterial assemblage and functional traits indicated that the habitat filtering and niche differentiation (treatment units) exerted selection on microbial communities based on functional traits, particular for key ecological functions related to nitrogen cycling. Collectively, our findings provide insights into structure-function associations at the local level and shed light on ecological rules guiding rDNA- and rRNA-based community assembly in landfill leachate treatment systems.

* Corresponding authors.
E-mail addresses: heyl@mail.xjtu.edu.cn (Y. He), weigehong@nwsuaf.edu.cn (G. Wei).

https://doi.org/10.1016/j.scitotenv.2018.07.388
0048-9697/

1. Introduction

Landfill leachate contains high concentrations of ammonium, sulfate, methane, dissolved organic carbon (as chemical oxygen demand, COD), dissolved inorganic carbon, and antibiotics (Wu et al., 2015; Zhang et al., 2017). Considering landfill leachate can jeopardize the recipient environment and requires the implantation of strict effluent regulations, cost-effective and energy-efficient treatment processes have been widely applied to remove COD, nitrogen and other pollutants (Delgado Vela et al., 2015; Kartal et al., 2013). A full-scale landfill leachate treatment plant (LLTP), including a series of biological treatment units, contains highly complex microbial communities, which play crucial roles in various pollutant removal (Liu et al., 2018). From this perspective, LLTP is an ideal engineered system to investigate habitat-specific communities, competition and mutualism of microorganisms, and metabolic profiles of pollutant-associated degradation bacteria such as nitrogen transformation (Del Moro et al., 2016). Nitrogen removal process in a typical LLTP involves various biological conversions, such as anaerobic ammonium oxidation (anammox), nitrification, dissimilatory nitrate reduction to ammonium (DNRA) and denitrification. These conversions are catalyzed by a series of functional genes, including hydrazine synthase (*Hzs*), hydrazine dehydrogenase (Hdh), archaea ammonia monooxygenase (AOA-*amoA*), ammonia monooxygenase (AOB-*amoA*), nitrite oxidoreductase (*nxrA*), periplasmic nitrate reductase (*napA*), membrane-bound nitrate reductase (*narG*), dissimilatory nitrate reductase (*nrfA*), copper-containing nitrite reductase (*nirK*), nitrite reductase (*nirS*), quinol-dependent nitric oxide reductase (*qnorB*), and nitrous oxide reductase (*nosZ*) (Kuypers et al., 2018). These marker-gene-based studies provided important insights into the functional genes in the microbial nitrogen cycling network. Hence, knowledge of microbial community assembly, functional traits and linkages with fluctuating treatment processes is not only essential for understanding their complex metabolisms, but also beneficial for promoting the flexibility and stability of biological systems by engineers (Ferrera and Sánchez, 2016).

Previous studies based on environmental DNA provided insights into the distribution of microbial communities in ecosystems (Ju and Zhang, 2015; Lu et al., 2012; Ye and Zhang, 2013), and highlighted the importance of bacterial associations and environmental heterogeneity to shape biodiversity patterns at global and regional levels (Delgado-Baquerizo et al., 2018). A few studies have reported the phylogenetic diversity of rDNA and rRNA in bioswale soil (Gill et al., 2017), forest soil (Baldrian et al., 2012), coastal ocean (Campbell et al., 2011), and anaerobic digestion reactor (Cerrillo et al., 2017). Although these studies effectively linked bacterial community structure to function traits in engineered wastewater treatment systems, they neither accounted for functional traits of active microbes nor determined particular functional genes of these microbial activities in relation to treatment unit selection. Moreover, how DNA- and RNA-based communities differ or factors underlying community variation among wastewater treatment units in microorganisms encoding nitrogen transformation pathways at the local level are not entirely known. Hence, it inspired us to think over these questions: whether rDNA- and rRNA-based communities exhibit contrasting patterns, and to what extend this discrepancy is determined by the treatment units or is driving forced by divergent of functional traits?

To fill the knowledge gap of structure-function-process relationships, this study presents the first attempt to explore potential activities of taxa, community assembly, and functional traits across landfill leachate treatment units. Specifically, the following key questions were addressed in the present study: (1) Do rDNA- and rRNA-based communities exhibit similar or different diversities at the local level, and which parts of rDNA-based communities are metabolically active in response to given habitats? (2) What are the co-occurrence patterns of rDNA- and rRNA-based communities, and do core taxa have higher incidences of intra-phylum association than inter-phylum associations at the rRNA level? (3) What are the frequencies of different nitrogen transformation pathways in treatment units, and what are the functional taxa encoding each nitrogen pathway?

2. Materials and methods

2.1. Description of landfill leachate treatment plant and sample collection

Detailed information is summarized in Method S1, Tables S1, S2, and Fig. S1. Generally, sludge samples were collected from Jiangcun Gou WWTP, which is a full scale landfill leachate treatment plant in Xi'an, Shaanxi, China. It treats approximately 1044.3 m^3 leachate per day with a COD concentration of average 22,898 mg L^{-1}. In this LLTP, the treatment system consisting of UASB (upflow anaerobic sludge blanket), A/O (anoxic/aerobic) and MBR (membrane bioreactor). The two stage A/O integrate process included the first denitrification tank, first nitrification tank, second denitrification tank, and second nitrification tank. The MBR systems involved ultrafiltration, nanofiltration, and reverse osmosis components. The sludge samples AD, FD, FN, SD, and SN were taken from the UASB reactor, first denitrification tank, first nitrification tank, second denitrification tank, and second nitrification tank, respectively. In addition, because the ultrafiltration, nanofiltration, and reverse osmosis components were the integrated systems, the sample ST were collected from the sludge thickener according to the sludge pipelines in the LLTP. Triplicate representative samples were taken from each units (Method S1). After the sludge samples were collected, they were immediately fixed in LifeGuard® Soil Preservation Solution (MOBio, Qiagen, USA) and stored at −80 °C for DNA and RNA extraction.

2.2. DNA and RNA extraction, cDNA synthesis, and high-throughput amplicon sequencing

Total DNA and RNA were extracted from 2.0 ml sludge samples using FastDNA® SPIN Kit for Soil (MP Biomedicals, Illkirch, France) and RNA PowerSoil® Total RNA Isolation kit (MOBio, Qiagen, USA), respectively. Purified RNA and complementary DNA (cDNA) were obtained according to the manufacturer's protocol. Then, genomic DNA and cDNA were amplified by PCR using primer set 515F and 806R for amplification of hypervariable V4 region. Finally, purified amplicons were sequenced on the Illumina HiSeq 2500 PE250 platform. All raw data generated for rDNA and rRNA are publicly available in NCBI SRA database under accession number SRR6206202. Following sequencing, all the raw sequences were processed in QIIME v1.9.1-dev under the default settings (Method S2). The samples from DNA library were named AS, FD, FN, SD, SN, and ST. cAS, cFD, cFN, cSD, cSN, and cST represent samples from cDNA library. Detailed description of alpha and beta diversity, taxon-habitat association patterns, and community network constructions are described in the Supporting information (Method S2).

2.3. Shotgun metagenomic sequencing and bioinformatics analysis

Genomic DNA extracted in triplicate for each sample was pooled and subjected to shotgun metagenomic sequencing on Illumina HiSeq 2500 platform (Methods S3). Reads assembly, gene prediction, and taxonomic classification were performed as described previously (Guo et al., 2016). For functional annotations, sequences of proteins in the non-redundant gene catalog were blasted against the KEGG, eggNOG, and CAZy databases using BLASTP with an E-value cut-off of 10^{-5}. Raw sequences for each sample were deposited into NCBI SRA under accession number SRR6206203.

To further investigate distribution patterns of nitrogen functional genes in landfill leachate treatment units, nitrogen functional gene databases were established by downloading protein sequences of the *AmoA*, *nirK*, *nirS*, *nosZ*, *nrfA*, *norB*, *napA*, and *narG* genes from RDP FunGene (http://fungene.cme.msu.edu) as well as *Hao*, *HzsA*, and *Hdh*

genes from NCBI nr (https://www.ncbi.nlm.nih.gov/protein). A read was assigned as a nitrogen functional gene if the BLASTP hit (with an E-value cut-off of 10^{-5}) had a sequence identity of >90% and an alignment length >150 bp. The reads per kilo-base pairs million (RPKM) value was then calculated for each functional gene. Finally, taxonomic assignments of key nitrogen metabolism enzymes were blasted against the NCBI NR database (18 June 2016) using BLASTX (version 2.3.0) (Method S3).

2.4. Quantitative real-time PCR

The gene copy numbers of bacteria 16S rRNA, anammox 16S rRNA, AOB *amoA*, AOA *amoA*, *nxrA*, *nirK*, *nirS*, *napA*, *narG*, *nrfA*, q*norB*, and *nosZ* in all the rDNA and rRNA samples were quantified using a Mastercycler ep realplex (Eppendorf, Hamburg, Germany) instrument based on the SYBR Green II method, according to our previous study (Shu et al., 2015). The primer pairs and protocols for qPCR were summarized in Table S2. Triplicate assays were conducted for each sample (Method S4).

3. Results and discussion

3.1. rRNA/rDNA ratios of microbial communities

For both natural and engineered ecosystem, key functional traits are driven by active communities (Gruber and Galloway, 2008). In order to understand the influences of environmental processes on microbial communities, the distinction between active and inactive is critical (Singer et al., 2017). Although rRNA cannot indicate in situ bacterial growth rates and real-time activity in environmental samples, rRNA can represent past, current, and future cellular activities under ex situ circumstances (Blazewicz et al., 2013). Therefore, the ratios of 16S rRNA and rDNA, inferred as an index of potential activity for specific taxa in WWTPs were measured by combining high-throughput 16S rRNA and rDNA sequencing analyses (Cerrillo et al., 2017).

A detailed sequencing summary is described in the Results and discussion of the Supporting information. The correlations between rRNA and rDNA frequencies for each assigned OTU across all sludge samples were determined. Of all the assigned OTUs, a positive correlation was observed between rDNA and rRNA frequencies (Kendall's nonparametric $\tau = 0.61$, $P < 0.001$; Spearman's rank correlation $r_s = 0.77$, $P < 0.001$; $n = 2660$) (Fig. 1a). Most local OTUs across all samples had a low abundance (<0.1%). Moreover, a considerable fraction of taxa was above the 1:1 line, which included OTUs affiliated with *Nitrospira* and *Anammox*-associated organism *Planctomyces* (Fig. 1b). In addition, several low abundance taxa had higher rRNA/rDNA ratios (>2) than that in the abundant taxa (Fig. S2a, b). These results were consistent with the findings of previous results (Vuono et al., 2016), indicating that relative abundances increase for some bacteria as their potential activities decrease.

In order to further corroborate the fact that the occurrence of a given microbe does not imply its activity, both abundant and rare taxa (Campbell et al., 2011) were defined in this study. Our results showed that abundant taxa have significantly lower rRNA/rDNA ratios than rare taxa (Figs. 1a, b and S2). Moreover, only 7.3% of microbial taxa was abundant, while 39.3% of rare taxa and 53.4% of transient taxa dominated most of the microbial diversity. However, the rRNA/rDNA ratios also indicated that 42.8% of rare taxa may be inactive or dormant. Previous studies showed that the rare taxa play pivotal roles in nutrient cycling, especially nitrogen cycling (Lawson et al., 2015). Compared with abundant taxa, the results in this study indicated that a considerable fraction of rare bacteria across landfill leachate treatment units maintained high potential activity levels (Fig. 1b). One potential explanation for this is that the abundant taxa are more preyed by bacteriophage predation (Shapiro et al., 2010).

Additionally, known nitrite oxidizing bacteria (NOBs) were affiliated to *Nitrospiraceae*, *Nitrosococcus*, *Nitrolancea*, and *Comamonas*; and anammox microorganisms were associated with *Planctomycetaceae*. Known ammonia oxidizing bacteria (AOBs) affiliated to *Nitrosomonas* and denitrifier associated taxa, such as *Nitratireductor*, *Pseudomonas*, *Thauera*, *Halomonas*, and *Hahella*, et al. (Fig. 1b). These microorganisms had persistently high activities in nitrification and denitrification treatment units, as well as in anaerobic treatment units. Therefore, anaerobic treatment units, which could serve as a microbial seed bank (Saunders et al., 2016), providing functional bacteria for nitrification and denitrification treatment units (Lettinga, 2014). Additionally, although NOB clades *Nitrospira* were rare, their rRNA/rDNA ratios were higher in the first nitrification treatment unit than that in other treatment units. These results highlight the importance of rare taxa as a large proportion of active taxa over abundant taxa in treatment units.

3.2. Divergent assemblage patterns of rDNA- and rRNA-based communities

Regarding the α-diversity indices, Shannon, Simpson, Chao1, ACE, and PD whole tree in the rDNA community were 1.2–1.7 folds higher than that in the rRNA community ($P < 0.05$) (Table S4). The average Good's coverages ranged from 99.2–99.5%, demonstrating that rDNA and rRNA communities can be covered by sequence libraries. Based on random subsampling, rarefaction curves showed that rDNA samples had a high α-diversity than rRNA samples (Fig. S4). *Alpha*-diversity estimators indicated that rDNA-derived communities have a greater evenness and richness of bacterial phylotypes compared to those rRNA-based communities (Table S4), inconsistent with newly reported studies (Gill et al., 2017). It seems that distinct diversity patterns appeared to be driven in part by the differences of treatment units.

Regarding β-diversity, PCoA based phyla abundance revealed a maximum variation of 52.1% (PCo1) and 21.1% (PCo2) for the rDNA community, and 85.6% (PCo1) and 5.4% (PCo2) for the rRNA community (Fig. 2a, c). Meanwhile, on the taxonomy level, compared with rDNA-based communities (ANOSIM, $R = 0.3695$, $P = 0.007$), samples from AS and ST were clearly separately from the nitrification-denitrification reactors (i.e. FD, SD, FN, and SN) (ANOSIM, $R = 0.2675$, $P = 0.013$). PERMANOVA confirmed the significant differences between rDNA- and rRNA-based communities, while both these bacterial communities did not have significant differences ($P > 0.05$) in the nitrification-denitrification reactors (Table S5). Additionally, ANOSIM and PERMANOVA analyses (Table S4) demonstrated that significant differences in anaerobic digester sludge samples and post-sludge thickener samples, although the variations between four samples from nitrification-denitrification components were not statistically significant ($P > 0.05$). Therefore, it is concluded that samples clustered within each treatment units, and bacterial assemblage following each unit operation.

The contrasting trends of potential activity between rDNA and rRNA communities result in divergent assemblage patterns of these bacterial communities. Although *Proteobacteria*, *Bacteroidetes*, *Firmicutes*, *Chloroflexi*, and *Planctomycetes* are the dominant phyla in the rDNA- and rRNA-derived communities, the degree of differentiation in rRNA-expressed communities could not be concluded from the total community patterns (Figs. 1c, d and S3). These uncoupled community structure estimates were driven by discrepancies in the relative abundance of major phylotypes based on whether RNA or DNA was examined. For example, in all of the treatment units, *Proteobacteria* were clearly the most abundant phyla among rDNA phylotypes, as well as the genera of Candidatus *Competibacter*, *Ottowia*, and *Nitrosomonas*. However, their abundances were lower than that in the rRNA-based communities, indicating that rank abundance of rDNA-derived communities may be misleading in respect to rRNA-derived community structures. Detailed information of assemblage patterns of rDNA- and rRNA-based communities is described in the Results section of the Supporting information. In general, from the perspective of taxonomy level, the bacterial

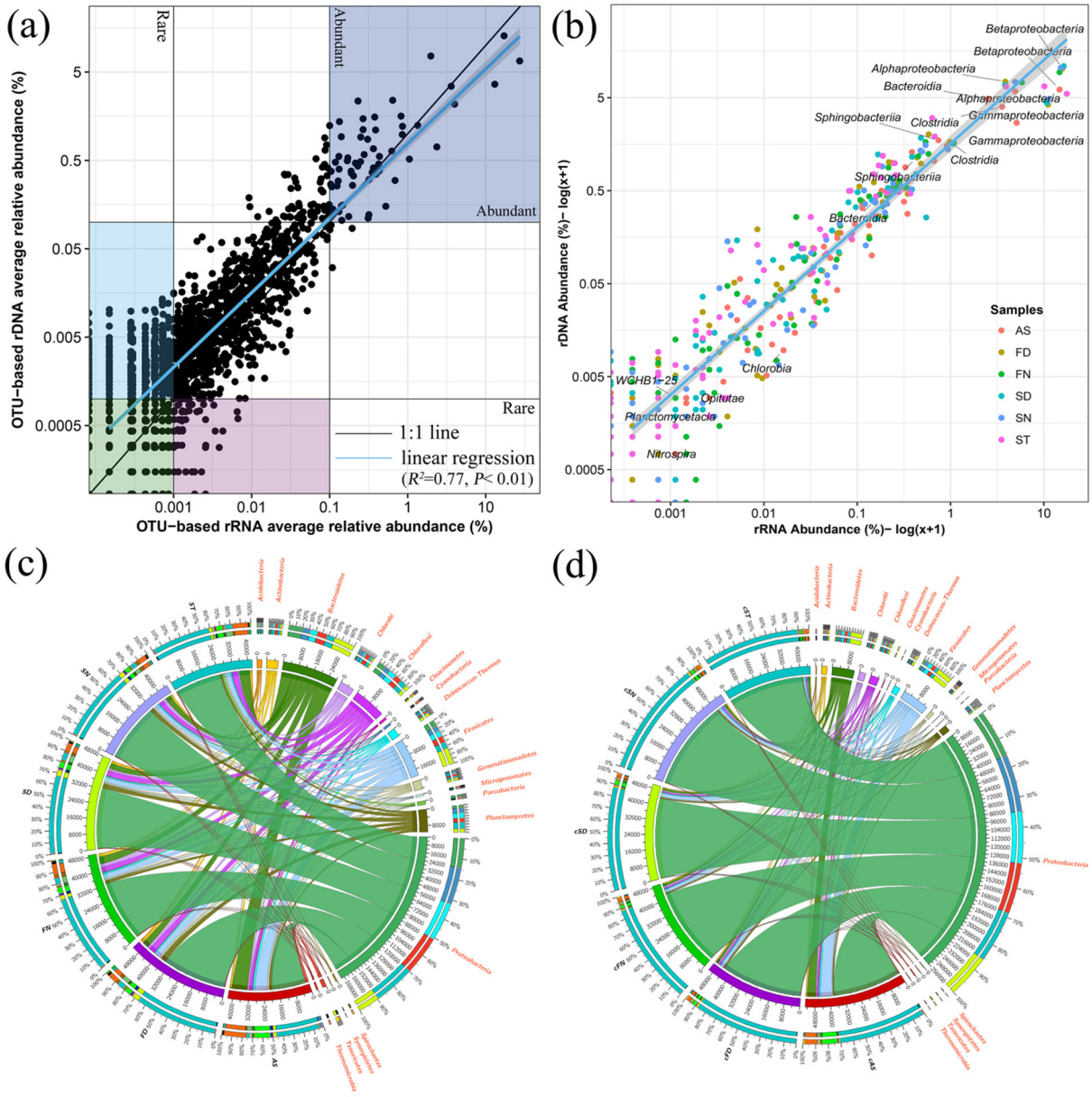

Fig. 1. Distribution of phyla in the rDNA (a) and rRNA (b) samples based on the taxonomy annotation via SILVA SSU database using QIIME. The thickness of each ribbon represents the abundance of each taxon. The absolute tick above the inner segment and relative tick above the outer segment stand for the reads abundances and relative abundance of each taxon, respectively. The data were visualized using Circos (Version 0.67, http://circos.ca/). (c) Average relative abundance of individual OTUs (dot) according to rRNA and rDNA. (d) Relationship between the rRNA and rDNA frequencies of bacteria OTUs at each treatment unit (AS, anaerobic sludge; FD, first denitrification unit; FN, first nitrification unit; SD, second denitrification unit; SN, second nitrification unit; ST, the sludge thicker unit).

assemblage patterns of rDNA- and rRNA-based communities differed substantially. For example, within *Proteobacteria*, *β-Proteobacteria* (15.2–28.6% in rDNA and 26.3–45.6% in rRNA) was the dominant class, followed by *γ-Proteobacteria* (6.4–13.5% in rDNA and 12.5–50.1% in rRNA) and *α-Proteobacteria* (14.4–18.7% in rDNA and 9.2–4.3% in rRNA). Results of the Wilcoxon rank sum tests indicated that assemblage patterns between rDNA- and rRNA-based communities have remarkable differences ($P < 0.05$) in the same treatment units. The possible explanation was that rDNA- and rRNA-based communities displayed different sensitivity to environmental variables.

However, our results suggest that the same pattern of bacterial communities in nitrification-denitrification stages (Peng et al., 2014), where bacterial community structures in LLTP were primarily shaped by anaerobic treatment unit operations. Although short and large time-series 16S rRNA (rDNA) from drinking water treatment plant (Ma et al., 2017) and full-scale wastewater treatment plants (Ju and Zhang, 2015) were analyzed, bacterial communities are less sensitive to temporal changes, such as seasonal succession. These results also indirectly revealed the temporal and dynamics of bacterial communities in this study following each treatment unit rather than season, and explained why we did not collect sludge samples from each treatment unit over time.

3.3. Taxon-habitat association patterns and indicator species through the LLTP trains

The directed network showed that 430 and 385 indicator OTUs were significantly associated ($q < 0.05$) with the rDNA and rRNA communities, respectively. For the rDNA community, most of indicator OTUs were affiliated to candidate phyla, including *Firmicutes*, *Proteobacteria*,

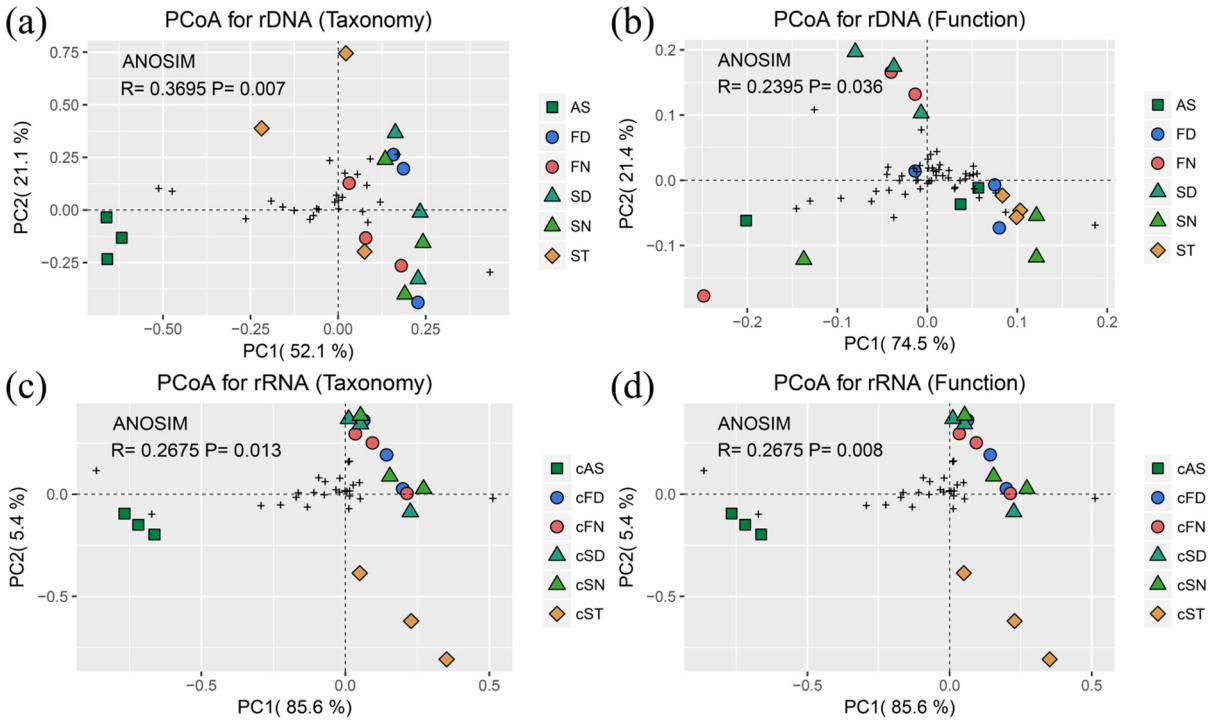

Fig. 2. (a) and (c) Different of taxonomy in rDNA- and rRNA-based communities shown by principal coordinate analysis ordinations (PCOs, based on weighted UniFrac distance matrices). (b) and (d) Different of function in rDNA- and rRNA-based communities shown by principal coordinate analysis ordinations (PCOs, based on weighted UniFrac distance matrices).

Chloroflexi, and *Planctomycetes* (Fig. 3a–b). For the rRNA community, the indicator OTUs had similar associated patterns. *Firmicutes* were the richest indicator phylum at the anaerobic sludge unit and accounted for 24.15% of the rDNA and 30.38% of the rRNA OTUs (Fig. 3c–d).

The bipartite association network resembled PCoA ordinations, demonstrating the major discriminative gradients related to indicator taxa and treatment units. The association strengths of indicator OTUs in the rDNA and rRNA communities ranged from 0.20–0.95 and 0.21–0.97, respectively, and 43 indicator OTU clusters were obtained in the bipartite network. Of these clusters, cluster 6 accounted for 60.4% and 62.4% of the indicator OTUs in the rDNA and rRNA communities, respectively, which were associated with cross-combinations of all treatment units. Clusters 2–31 and cluster 2–30 accounted for 92.1% of the rDNA and 57.7% of the rRNA indicator OTUs, respectively, which were most strongly associated with two or more treatment units. Additionally, Cluster 1, 37 and 43 were most strong associated with only one treatment unit in the rDNA community, as well as the Cluster 1 and 39 in the rRNA community (Fig. S5a, b).

Among the indicator OTUs, the most representative OTUs affiliated to *Firmicutes* were positively associated with AS and cAS samples. For the rDNA community, the representative genera *Ruminococcaceae*, *Caldicoprobacter*, *Ruminiclostridium*, *Fusibacter*, and *Anaerovorax* were especially prominent in the ST sample. Indicator OTUs associated with samples from denitrification and nitrification tanks, including FD, FN, SD, and SN, were affiliated to various phyla, such as *Firmicutes*, *Actinobacteria*, *Microgenomates*, *Acidobacteria*, and *Proteobacteria*. However, some discrepant patterns appeared in the rRNA community. For instance, indicator OTUs affiliated to *Spirochaetes*, *Ruminiclostridium*, *Candidatus Odyssella*, and *Candidatus Competibacter* were specifically prominent in cST samples. In addition, a sizeable proportion of indicator OTUs associated with FD, FN, SD, and SN samples were affiliated to various phyla, including *Deferribacteres*, *Chlorobi*, *Tenericutes*, and *Proteobacteria* (Fig. S6a, b). Although other OTUs associated with each treatment step were scattered across the taxonomic tree, some indicators OTUs revealed a strong response to anaerobic sludge thickener. Furthermore, the taxa-habitat association patterns (Figs. S5, S6) demonstrate that the anaerobic treatment and the first nitrification treatment habitats made greater contributions to bacterial community assemblages. Therefore, it is reasonably concluded that rRNA-derived communities are more sensitive to different habitats, and the anaerobic and first nitrification habitats could have acted as a microbial seed bank (Lennon and Jones, 2011) in this study.

To further explore the effect of habitats on the rDNA- and rRNA-derived communities, the Spearman's correlations between selected environmental factors and indicators OTUs were calculated (Fig. S8). At the genus level, 24 selected indicator OTUs at rDNA level affiliated to *Actinobacteria*, *Bacteroidetes*, and *Proteobacteria*, etc. were positively correlated with DO, influent pH, effluent pH, influent NO_2^--N, effluent NO_2^--N, and influent NO_3^--N. In rRNA-derived communities, 30 selected indicator OTUs affiliated to *Bacteroidetes*, *Thermotogae*, *Firmicutes*, and *Proteobacteria* were positively correlated with DO, influent pH, influent NO_2^--N, and effluent NO_2^--N, whereas influent NO_3^--N and NH_4^+-N were positively correlated with OTUs that affiliated to various genera, including *Sulfurospirillum*, *Proteiniphilum*, and *Nitrolancea*.

These results indicated that wastewater treatment characteristics and operational parameters (such as DO, temperature, HRT, and MLVSS) were important environmental attributes for shaping rDNA- and rRNA-based communities. However, although different environmental attributes derived distinct rDNA- and rRNA-based communities, pH, DO, NO_2^--N, and NO_3^--N were also the key drivers in guiding both rDNA- and rRNA-based communities assembly (Fig. S8). Previous studies showed that pH and DO have strong correlations with bacterial community variance (Wang et al., 2016), and our results support this association at rDNA and rRNA levels. Furthermore, our results indicated that operational parameters had a stronger correlation with anaerobic sludge samples, whereas wastewater characteristics had positively association with nitrification and denitrification treatment units (Fig. 2). Collectively, environmental heterogeneity (or niche differentiation) has a prominent role in guiding the assembly and dynamics of rDNA- and rRNA-based communities, consistent with previous studies (Ju

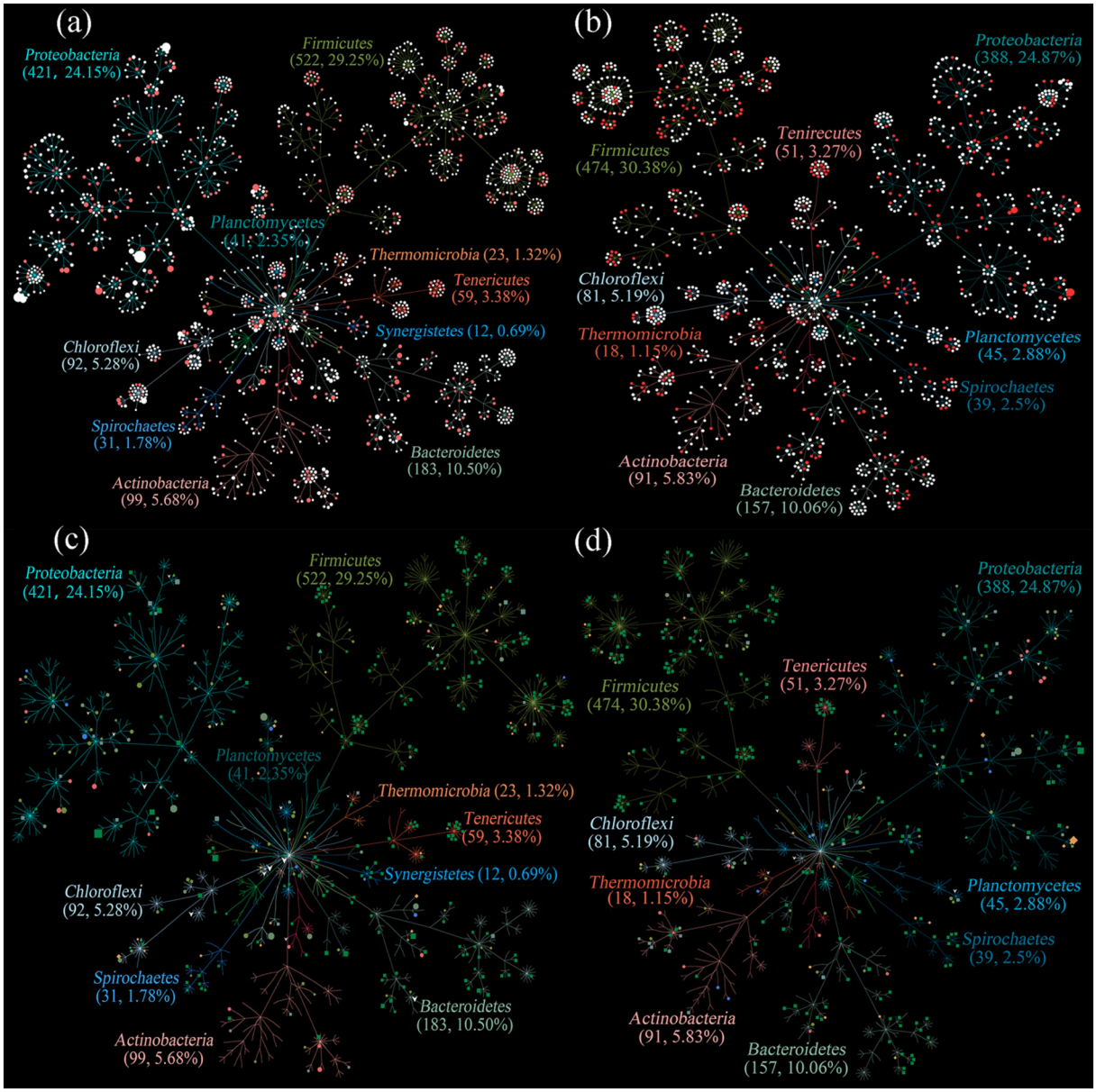

Fig. 3. (a) and (b) Taxonomic dendrograms of the detected rDNA- and rRNA-based communities showing the OTU distribution across the different taxonomic branches (colour coded by phylum). Nodes correspond to OTUs and node sizes correspond to their relative abundances (square root) in the data set. Edges represent the taxonomic path from the root to OTU level and OTUs were placed at the level of the lowest possible assignment. Red nodes correspond to OTUs that significantly ($q < 0.05$) differed among each treatment step, whereas white nodes represent insensitive OTUs. (c) and (d) Only the significant OTUs ($q < 0.05$) colour coded according to the each treatment step association in rDNA- and rRNA-based communities, respectively. OTUs colour and symbol coded according to Fig. 2.

et al., 2017; Ju and Zhang, 2015; Sun et al., 2014), and these findings are further supported at the rRNA level in the present study.

3.4. Microbial co-occurrence network and network topological features

In engineered ecosystems, microorganisms live together within networks through positive (i.e., commensalism and mutualism) and negative (amensalism and competition) interactions (Deng et al., 2016). In the present study, the core sub-network and global network were constructed for core taxa and whole community, respectively. Topological features, including betweenness, closeness, eigenvector centrality, and node degree were calculated on the base of unique node-level (Fig. 4, Table S6). The positive links of core sub-network in rRNA-based community were significantly more than those in rDNA-based community, indicating that rDNA had more inter-species competition. In addition, the value of closeness, eigenvector centrality, and node degree in rRNA community network were greater than that in rDNA community network except betweenness (Fig. 4c–f). The results indicated that rRNA-based community had more robust associations (Ju and Zhang, 2015), although the genera affiliated with rDNA-based community were more widely distributed.

Additionally, the global rDNA community network contained 187 nodes (genera) and 210 edges. The rRNA community network comprised 195 nodes and 591 edges. Topological features, including the observed modularity (MD: 0.91), clustering coefficient (CC: 0.66), and average path length (APL: 3.52) in the OUT-based rDNA network and MD (0.68), CC (0.82), and APL (4.26) in the rRNA network, demonstrating that both the rDNA and rRNA networks have modular structures (Table S5). Likewise, the value of closeness, eigenvector centrality, and node degree in rRNA community network were greater than that in

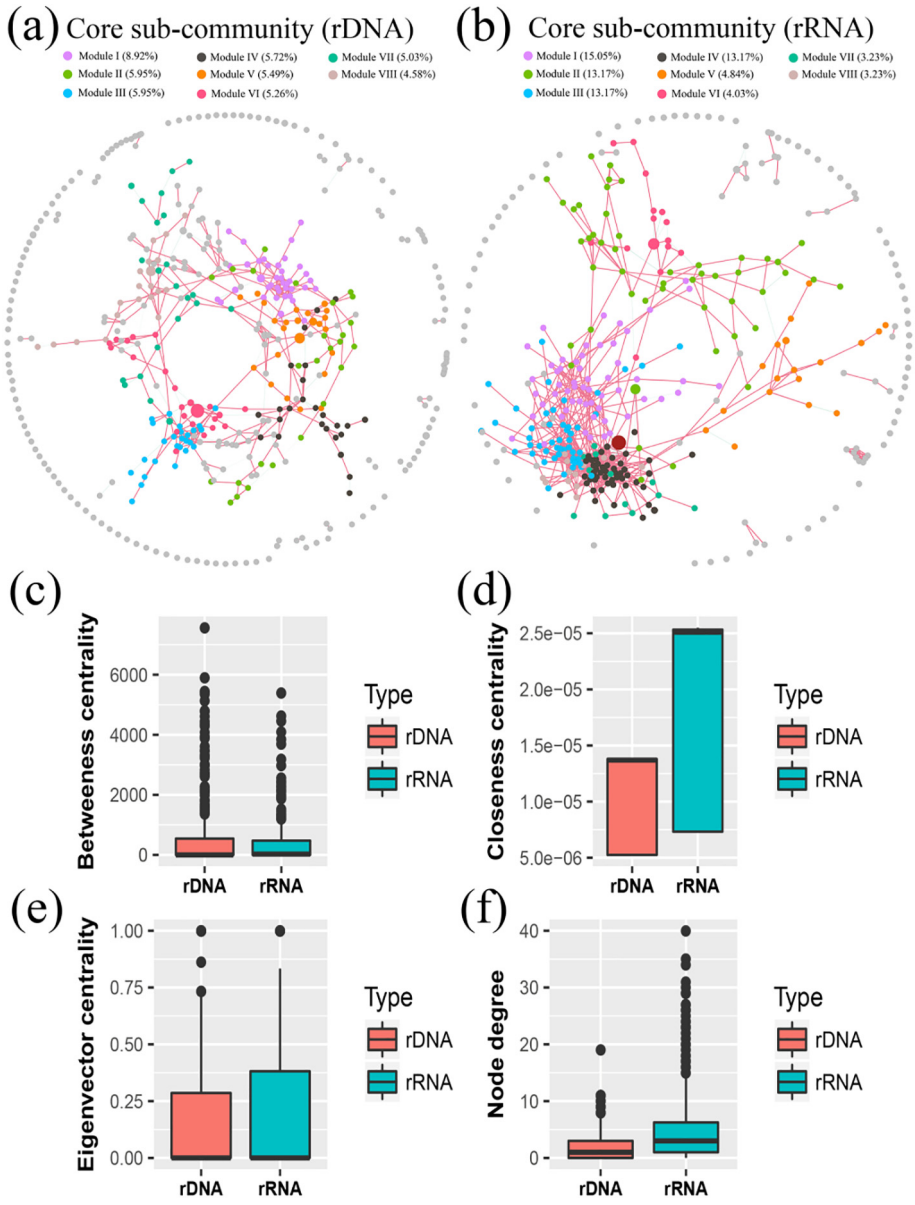

Fig. 4. Network of co-occurring bacterial core sub-community in landfill leachate treatment systems, based on correlation analysis. Each edge stands for a strong ($\rho > 0.6$) and significant correlation ($q < 0.05$). The size of each node is proportional to the relative of phylum. The thickness of the edges is proportional to each phylum of Spearman's correlation coefficient. (a) and (b) Represent the co-occurring network coloured by phylum in rDNA- and rRNA-derived core sub-communities, respectively. The node-level topological features of different rDNA- and rRNA-derived core sub-communities, namely betweenness (c), closeness (d), centrality (e), and degree (f) the co-occurring network coloured by modularity class in rDNA- and rRNA-derived core-communities, respectively.

rDNA community network except betweenness. Moreover, the positive correlations in RNA network were higher than that in rDNA network (Fig. S7c, f). At the genus level, although the degree of intra-phylum co-occurrence varied, *Firmicutes*, *Bacteroidetes* and *Actinobacteria* displayed high incidences of inter-phylum positive association. In addition, *Proteobacteria* and other phyla presented widespread correlations with other bacterial genera. Furthermore, both rDNA and rRNA positive networks could be clustered into eight major modules based on the modularity class. Among these modules, 22 of 37 rDNA vertices and 81 of 155 rRNA vertices occupied the three largest modules, modules I, II and III (Fig. S7).

Taken together, as revealed by the co-occurrence network, substantial differences were observed between rRNA- and rDNA-derived communities (Table S6, Figs. 4 and S7). Modularity index of core sub-network (>0.4) indicate that both rRNA- and rDNA-based communities have modularity structure (Barberán et al., 2012). Compared with random network, results of average path length and clustering coefficient suggest that observed core sub-network and whole network had "small world" properties (Hu et al., 2018; Zhang et al., 2018).

When it comes to topological features, a previous study revealed that high betweenness centrality values represent a core location of this sub-network in the whole community network (Ma et al., 2016). As present in the Figs. 1c and S7c, our results suggest that core taxa (Gülay et al., 2016) from rDNA-based communities were more located in central positions within the whole network than rRNA-based communities. However, it was observed that rRNA-based communities had higher closeness centrality, node centrality and node degree, indicating that more interactions and closer relationships for rRNA-based communities than that for rDNA-based communities. Moreover, the higher positive correlations and lower negative associations in core

sub-network and global network suggest that more mutualism or cooperation of core taxa which affiliated with rRNA-based communities. In contrast, core taxa from rDNA-based communities had more competition or amensalism linkages. These competitive associations could explain why abundant taxa are low activity in rDNA-based communities.

Although the rDNA-based community had a modular structure, incidences of inter-taxa co-occurrence between *Firmicutes*, *Proteobacteria*, *Bacteroidetes*, and other pairs of phyla were also observed in the global network. The results were essentially consistent with observations of taxa in activated sludge of globally distributed WWTPs in previous studies, revealing that ecological interactions have an important influence on rDNA-based community assembly (Ju et al., 2014). By contrast, rRNA-based community was found to have higher incidence of strong intra-phylum co-occurrence associations and higher clustering coefficients (Fig. S7a, b). For example, *Firmicutes* and *Bacteroidetes* showed strong intra-phylum co-occurrence, which is similar with previous studies showing that bacterial communities in soil (Delgado-Baquerizo et al., 2018) and WWTPs (Griffin and Wells, 2017) are phylogenetically clustered. One explanation for this is that the taxonomically closely related genera are closely related ecologically (i.e., existence of non-exclusive mechanisms), and these taxa share similar habitat preferences (Ju et al., 2017). Another explanation for discrepancies of ecological linkages is the differences functional traits of the rDNA- and rRNA-based communities (Hua et al., 2015).

3.5. Nitrogen metabolic pathways and taxonomic origins of the functions in nitrogen metabolism

In this study, nitrogen-cycling-related functional gene abundance and gene expression was explored using qPCR. Results showed that functional gene distribution (Figs. 5, S9) and relative transcriptional activity (Fig. S10) differed substantially. On the base of Pearson's correlation (Table S7), results indicated that coupling of anammox, denitrification and DNRA accounted for nitrogen removal in the landfill leachate system. A detailed discussion of abundant taxa can be found in the Results and discussion section of the Supporting information.

Additionally, metabolic pathways associated with the nitrogen cycle, including nitrification, denitritation, denitrification, dissimilatory N reduction and anammox were further analyzed based on metagenomic sequencing. Subunits of gene, *Hao*, *nosZ*, *norB*, and *nirS*, encoding nitrification and denitrification had higher abundance across the whole metagenomic dataset. Specifically, most subunits of nitrogen-cycling-related genes were highly abundant in AS samples (Fig. 6).

For the nitrification process, *amoA* and *Hao* subunits were abundant genes in the first denitrification (FD) and nitrification (FN) treatment units, with average hit reads of 517 and 2505 for FD and FN, respectively. In the denitritation process, the *napA* and *narG* genes were the most abundant with 649 and 249 hit reads in the first nitrification treatment unit. The *nrfA* genes had relatively lower numbers of hit reads in the four samples from first and second nitrification-denitrification treatment units. In the denitrification process, the conversions of NO_2^--N to NO, N_2O, and finally, to N_2 are catalyzed by the *nirS*, *nirK*, *norB*, and *nosZ* subunits. Most of these genes, except for *nirK* in the FN and SN samples, were detected in high abundance in the first and second nitrification treatment units. Regarding the anammox process, *Hzs* gene, catalyzing the conversion of NH_4^+-N + NO_2^--N → N_2H_4 (Kartal et al., 2013), was detected in all sludge samples. Notably, the abundances of this gene in FN and SD samples were higher than those in FD and SN samples. The *Hdh* gene, the key enzyme that catalyses the conversion of N_2H_4 toN_2, had 607 and 405 hit reads in FD and FN samples, respectively. In addition, although this gene was detected in SD and SN samples, the abundances were relatively low at 399 and 365 hit reads, respectively.

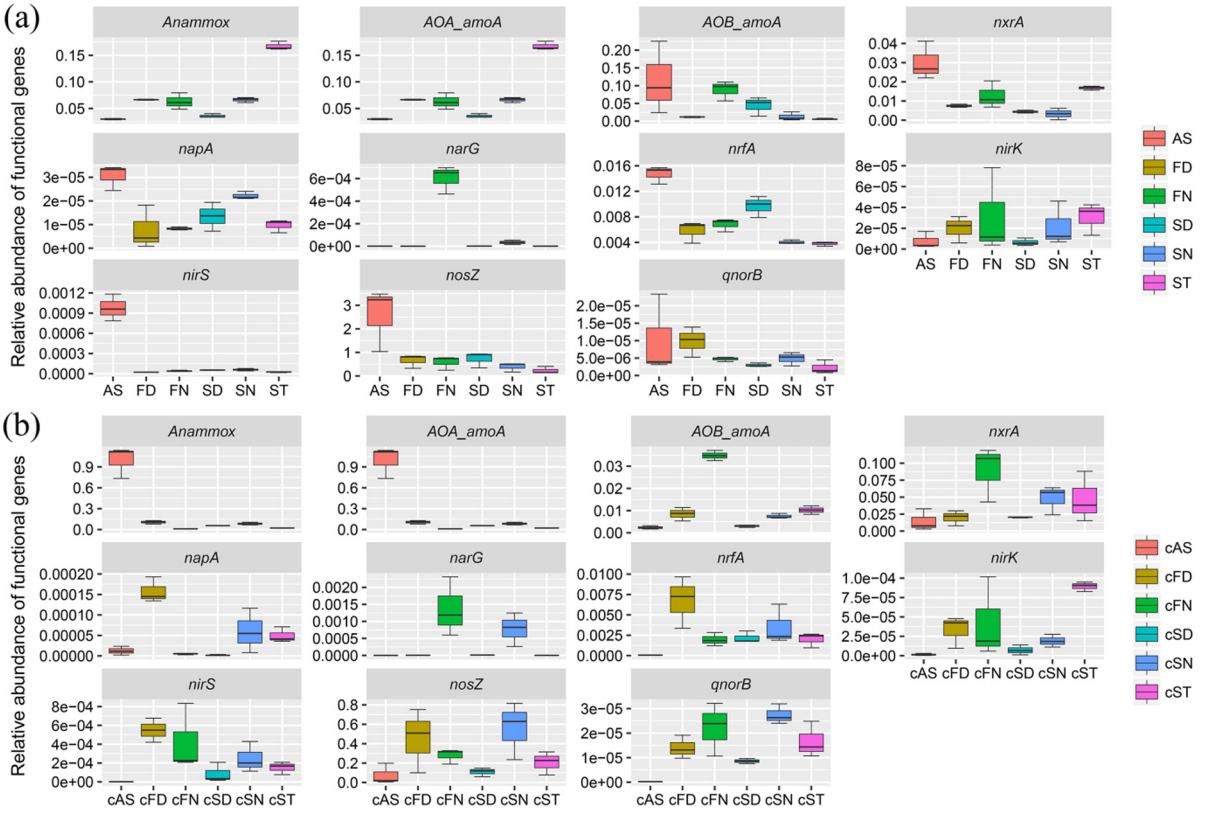

Fig. 5. Relative abundance of nitrogen-cycling-related genes in the rDNA and rRNA sludge samples based on the qPCR. For example, relative abundance of anammox represent the absolute abundance of anammox/absolute abundance of total bacteria. Error bars represent standard deviation calculated from three independent experiments.

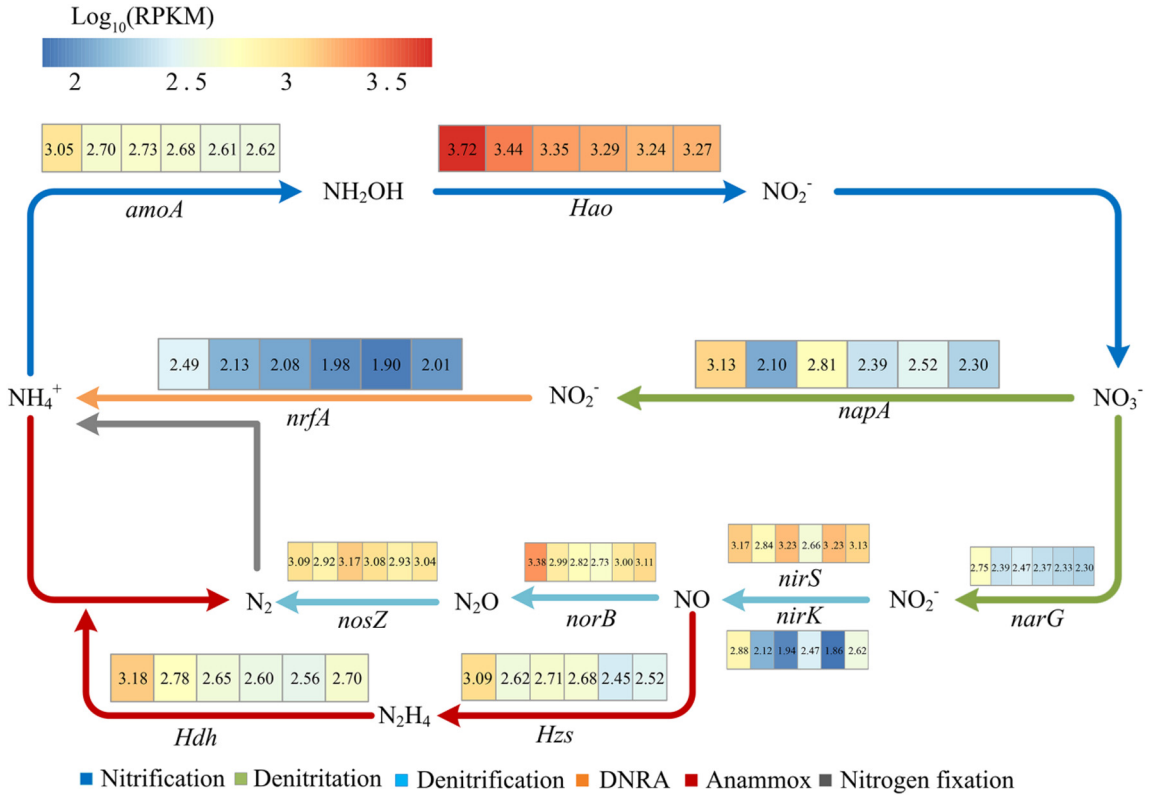

Fig. 6. Abundance of key enzymes for nitrification, denitritation, denitrification, dissimilatory nitrate reduction to ammonium, and anammox. Nitrogen pathways and key enzymes are coloured differentially. The abundance of the enzymes in each treatment step is shown in the horizontal colour bars. The order of each treatment step in horizontal colour bars from left to right is anaerobic sludge, the first denitrification unit, the first nitrification unit, the second denitrification unit, the second nitrification unit, and the sludge thicker unit. RPKM, hit reads per kilo-base pairs per one million reads.

Regarding taxonomic origins of functional genes primarily response for the nitrogen cycling process, anammox process was determined to be conducted by four genera *Candidatus Jettenia*, *Candidatus Scalindua*, *Candidatus Brocadia*, and *Candidatus Kuenenia*. Bacterial *amoA* and *Hao* were associated mostly with *β*- and *γ-proteobacteria* (e.g., *Comamonas*, *Nitrospira*, *Nitrosomonas*, and *Nitrosococcus*). Likewise, the denitritation process, mediated by *napA* and *narG*, was mainly annotated by *α*-, *β*- and *γ-proteobacteria* (e.g., *Acidovorax*, *Candidatus Competibacter*, and *Thauera*). In addition, the *nirK* gene in all samples was mostly associated with *Truepera*, *Geobacter*, and *Geopsychrobacter*, whereas the *nirS* gene was associated with *Acidovorax* and *Candidatus Accumulibacter*. The denitrification process, mediated by *norB* and *nosZ*, was mainly associated the phyla *Bacteroidetes*, *Proteobacteria*, and *Chloroflexi*. Notably, anammox and DNRA were functionally associated with the same bacteria genera. Additionally, other individual genera, including *Aeromonas*, *Ferrimonas* and *Shewanella* were associated with only the DNRA pathway (Fig. S11). These results suggest that a diverse range of bacteria are responsible for nitrogen cycling in landfill leachate treatment systems. Moreover, these results also revealed that particular nitrogen pathways in landfill leachate treatment operation units could be dominant by various groups, even including presently unknown rare and transient taxa that were previously considered unable to participate in nitrogen transformation pathway (Guo et al., 2016; Saunders et al., 2016).

3.6. Functional traits and ecological associations between nitrogen-cycling related genes

As shown in Fig. 2b and d, the functional profiles of the rDNA-based communities (ANOSIM, $R = 0.2395$, $P = 0.036$) overlapped more as compared to the rRNA-based communities (ANOSIM, $R = 0.2675$, $P = 0.008$). The PCoA of functional profiles of the nitrification-denitrification treatment units (included FD, SD, FN, and SN) showed higher similarity (Table S8), while functional profiles of the samples (AS and ST) differed significantly. Additionally, based on the shotgun metagenomic sequencing, KEGG, eggNOG, and CAZy functional clustering showed partial similarity among the FD, FN, SD, and SN samples, whereas significant discrepancies were observed between the AS and ST samples (Fig. S12). Based on level 3 KEGG subsystem and level 1 eggNOG subsystem analyses, these metabolic pathways involved carbon metabolism, amino acid biosynthesis, aminoacyl-tRNA biosynthesis, TCA cycle, fatty acid degradation, methane metabolism, and cell cycle caulobacter were more abundant in the FD, FN, SD, and SN samples relative to that in the ST sample, whereas its abundance was lower than that in the AS sample. By contrast, the FD, FN, SD, and SN samples had more inorganic ion transport, cell wall, cell motility, and nitrogen metabolism genes than the AS sample, whereas the sample abundances of these genes were lower than those in the ST sample (Fig. S13a, b). Moreover, functional profiles of AS and ST different significantly, while samples from nitrification or denitrification treatment units were clustered together (Fig. S13c, d).

In addition to AS and ST samples, there was similarity between nitrification and denitrification units (Fig. 2a, c), suggesting that convergence took place in the nitrification- denitrification units as a potential selective effect of the habitats. ANOSIM confirmed that this is particularly true for the functional traits (Fig. 2b, d and Table S8). However, there were significant effects between rDNA- and rRNA-based communities as well as different treatment units both on the basis of community structures and functional traits. Previous study (Ma et al., 2017) also reported that a selective change in the bacterial community assemblage, and treatment units contribution to this. Our results corroborated these findings on the functional level, especially on the RNA level.

Moreover, it was observed that less significant differences in β-diversity in rDNA-based communities that that in rRNA-based communities (Table S5). These results point to the selective power of the habitats in the guiding the assembly of rRNA-based communities. In addition, the variance among treatment units appeared to be smaller in the rRNA-based communities than in the rDNA-based communities, suggesting that considerable overlap in active microorganisms' functional capabilities in bacterial communities with divergent diversity, especially for nitrification and denitrification system. Hence, based on the 16s rDNA and rRNA sequencing, our results regarding both bacterial assemblage and functional traits indicated that the treatment units exert selection on the bacterial community based on functional traits.

Regarding the particular functional traits (Yan et al., 2017), such as ABC transporters, Aminoacyl-tRNA biosynthesis and Nitrogen metabolism, which were over-represented in the rDNA- and rRNA-based communities. Previous studies have also reported that some of these functional traits play central roles in maintaining the relatively stable microbial community (Guo et al., 2016; Lawson et al., 2017). Consistently with our study, nitrogen metabolism was found to be of great importance in the engineered treatment system. Therefore, we focused nitrogen-cycling related genes to gain insight of the functional selection and ecological association in the landfill leachate treatment system.

In the nitrification process units, AOA *amoA*, AOB *amoA*, and *nxrA* are the key genes responsible for the conversion of NH_4^+-N → NO_2^--N → NO_3^--N, carried out by the genera *Comamonas*, *Nitrospira*, and *Nitrosomonas*. AOA and AOB consumed NH_4^+-N and provided the substrate NO_2^--N for the *nxrA* gene, indicating that AOA, AOB and NOB partially cooperate in a beneficial manner.

In the first step of denitrification, the conversion of NO_3^--N → NO_2^--N, catalyzed by *narG* and *napA* reductase and carried by *Acidovorax*, *Candidatus Competibacter*, and *Thauera*, etc., provided the substrate NO_2^--N for the anammox conversion (NH_4^+-N + NO_2^--N → N_2). Notably, anammox-related bacteria, including *Candidatus Jettenia*, *Candidatus Scalindua*, *Candidatus Brocadia*, and *Candidatus Kuenenia*, were detected across all treatment units, indicating their metabolic versatility. This is consistent with previous studies (Huang et al., 2014; Kartal et al., 2013), providing evidence of the metabolic variety and adaptability of anammox bacteria in different niches. It is reasonable to conclude that AOB, denitritation and anammox bacteria have a mutually beneficial protocooperation, like previous observations in the partial denitrification-anammox process (Du et al., 2017).

The *nrfA* gene, catalyzing the conversion of NO_3^--N → NO_2^--N → NH_4^+-N, is often used as a gene marker for the DNRA pathway and is carried out by the genera *Aeromonas*, *Ferrimonas*, and *Shewanella*, etc. The *nirK* and *nirS* genes are key genes for the conversion of NO_2^--N to NO and are distributed in *Truepera*, *Geobacter*, and *Candidatus Accumulibacter*, etc. Previous study showed that high COD/N ratios favoured the DNRA process, whereas denitrifying bacteria favoured low COD/N ratios (van den Berg et al., 2015). Hence, parts of organic carbon are eliminated in the DNRA process and provide a comfortable ecological niches for denitrification, indicating that mutualism between the DNRA pathway and denitrifying bacteria plays a pivotal role in the removal of organic matter (Castro-Barros et al., 2017).

In the final two steps of denitrification, the conversions of NO → N_2O and N_2O → N_2 were performed by the *qnorB* and *nosZ* genes, respectively. These two genes carried out by different phyla. The *narG*, *napA*, *nirK*, and *nirS* genes provided the indirect or direct substrates for the *qnorB* and *nosZ* genes, revealing that positive associations among closely related denitrifiers are usually established based on synergistic relationships (Wang et al., 2017).

Given the these ecological associations, these findings suggest that not only do nitrification and denitrification processes play key roles in nitrogen removal but also that coupling of denitrification, DNRA and anammox processes are important pathways contributing to nitrogen loss in LLTP, which was also observed in tidal flow constructed wetland (Zhi et al., 2015).

4. Conclusion

To the best of our knowledge, this is the first study to investigate the selections of landfill leachate treatment units on rDNA- and rRNA-derived communities, functional traits, and expression of nitrogen-cycling-related genes. rDNA- and rRNA-derived communities present contrasting community structures and assemblage patterns. rRNA/rDNA ratios suggest that although abundance follows activity in a large proportion of taxa, 57.2% of rare taxa are active, and their potential activities increase as abundance decrease. Taxa-habitat association and co-occurrence network showed taxonomically closely related taxa are also closely related ecologically, elucidating that non-random intra-taxa associations, such as mutualism and commensalism, have an important impact on the assembly of rRNA-derived communities. Furthermore, in view of structure-functional relationship, treatment units selected microbes with particular genes related to functional traits, resulting in the discrepancies of microbial assemblages. Especially for nitrogen metabolism, our results suggest that coupling of denitrification, DNRA and anammox processes are important pathways accounting for nitrogen removal in LLTP. However, to what extent nitrogen related functional traits is controlled by the treatment units needs further study using ^{15}N-labeled ammonium-based isotopic-tracing and metatranscriptomics.

Supplementary data to this article can be found online at https://doi.org/10.1016/j.scitotenv.2018.07.388.

Acknowledgements

This study was financially supported by National Science Foundation of China (41701291), China Postdoctoral Science Foundation (2017M620473), Ph. D start-up fund of Northwest A & F University (Z109021641), and Youth Elite Project of Northwest A & F University (Z109021805). We gratefully thank Qingyi Wang for assistance with sample collection. We acknowledge Martin Hartmann (Rhizosphere Processes Group, Swiss Federal Research Institute WSL, Birmensdorf, Switzerland) for his assistance with directed and bipartite association networks.

References

Baldrian, P., Kolařík, M., Štursová, M., et al., 2012. Active and total microbial communities in forest soil are largely different and highly stratified during decomposition. ISME J. 6 (2), 248–258.
Barberán, A., Bates, S.T., Casamayor, E.O., et al., 2012. Using network analysis to explore co-occurrence patterns in soil microbial communities. ISME J. 6 (2), 343–351.
Blazewicz, S.J., Barnard, R.L., Daly, R.A., et al., 2013. Evaluating rRNA as an indicator of microbial activity in environmental communities: limitations and uses. ISME J. 7 (11), 2061–2068.
Campbell, B.J., Yu, L., Heidelberg, J.F., et al., 2011. Activity of abundant and rare bacteria in a coastal ocean. Proc. Natl. Acad. Sci. 108 (31), 12776–12781.
Castro-Barros, C.M., Jia, M., van Loosdrecht, M.C., et al., 2017. Evaluating the potential for dissimilatory nitrate reduction by anammox bacteria for municipal wastewater treatment. Bioresour. Technol. 233, 363–372.
Cerrillo, M., Viñas, M., Bonmatí, A., 2017. Unravelling the active microbial community in a thermophilic anaerobic digester-microbial electrolysis cell coupled system under different conditions. Water Res. 110, 192–201.
Del Moro, G., Prieto-Rodríguez, L., De Sanctis, M., et al., 2016. Landfill leachate treatment: comparison of standalone electrochemical degradation and combined with a novel biofilter. Chem. Eng. J. 288, 87–98.
Delgado Vela, J., Stadler, L.B., Martin, K.J., et al., 2015. Prospects for biological nitrogen removal from anaerobic effluents during mainstream wastewater treatment. Environ. Sci. Technol. Lett. 2 (9), 234–244.
Delgado-Baquerizo, M., Oliverio, A.M., Brewer, T.E., et al., 2018. A global atlas of the dominant bacteria found in soil. Science 359 (6373), 320–325.
Deng, Y., Zhang, P., Qin, Y., et al., 2016. Network succession reveals the importance of competition in response to emulsified vegetable oil amendment for uranium bioremediation. Environ. Microbiol. 18 (1), 205–218.
Du, R., Cao, S., Li, B., et al., 2017. Performance and microbial community analysis of a novel DEAMOX based on partial-denitrification and anammox treating ammonia and nitrate wastewaters. Water Res. 108, 46–56.
Ferrera, I., Sánchez, O., 2016. Insights into microbial diversity in wastewater treatment systems: how far have we come? Biotechnol. Adv. 34 (5), 790–802.

Gill, A.S., Lee, A., McGuire, K.L., 2017. Phylogenetic and functional diversity of total (DNA) and expressed (RNA) bacterial communities in urban green infrastructure bioswale soils. Appl. Environ. Microbiol. https://doi.org/10.1128/AEM. 00287-17.
Griffin, J.S., Wells, G.F., 2017. Regional synchrony in full-scale activated sludge bioreactors due to deterministic microbial community assembly. ISME J. 11 (2), 500–511.
Gruber, N., Galloway, J.N., 2008. An Earth-system perspective of the global nitrogen cycle. Nature 451 (7176), 293.
Gülay, A., Musovic, S., Albrechtsen, H.-J., et al., 2016. Ecological patterns, diversity and core taxa of microbial communities in groundwater-fed rapid gravity filters. ISME J. 10 (9), 2209.
Guo, J., Peng, Y., Fan, L., et al., 2016. Metagenomic analysis of anammox communities in three different microbial aggregates. Environ. Microbiol. 18 (9), 2979–2993.
Hu, J., Zhao, F., Zhang, X.-X., et al., 2018. Metagenomic profiling of ARGs in airborne particulate matters during a severe smog event. Sci. Total Environ. 615, 1332–1340.
Hua, Z.-S., Han, Y.-J., Chen, L.-X., et al., 2015. Ecological roles of dominant and rare prokaryotes in acid mine drainage revealed by metagenomics and metatranscriptomics. ISME J. 9 (6), 1280.
Huang, X., Gao, D., Tao, Y., et al., 2014. C2/C3 fatty acid stress on anammox consortia dominated by "*Candidatus Jettenia asiatica*". Chem. Eng. J. 253, 402–407.
Ju, F., Zhang, T., 2015. Bacterial assembly and temporal dynamics in activated sludge of a full-scale municipal wastewater treatment plant. ISME J. 9 (3), 683–696.
Ju, F., Xia, Y., Guo, F., et al., 2014. Taxonomic relatedness shapes bacterial assembly in activated sludge of globally distributed wastewater treatment plants. Environ. Microbiol. 16 (8), 2421–2432.
Ju, F., Lau, F., Zhang, T., 2017. Linking microbial community, environmental variables, and methanogenesis in anaerobic biogas digesters of chemically enhanced primary treatment sludge. Environ. Sci. Technol. 51 (7), 3982–3992.
Kartal, B., Almeida, N.M., Maalcke, W.J., et al., 2013. How to make a living from anaerobic ammonium oxidation. FEMS Microbiol. Rev. 37 (3), 428–461.
Kuypers, M.M., Marchant, H.K., Kartal, B., 2018. The microbial nitrogen-cycling network. Nat. Rev. Microbiol. https://doi.org/10.1038/nrmicro.2018.9.
Lawson, C.E., Strachan, B.J., Hanson, N.W., et al., 2015. Rare taxa have potential to make metabolic contributions in enhanced biological phosphorus removal ecosystems. Environ. Microbiol. 17 (12), 4979–4993.
Lawson, C.E., Wu, S., Bhattacharjee, A.S., et al., 2017. Metabolic network analysis reveals microbial community interactions in anammox granules. Nat. Commun. 8, 15416–15423.
Lennon, J.T., Jones, S.E., 2011. Microbial seed banks: the ecological and evolutionary implications of dormancy. Nat. Rev. Microbiol. 9 (2), 119–130.
Lettinga, G., 2014. My Anaerobic Sustainability Story. LeAF Publisher, Wageningen.
Liu, J., Tian, Z., Zhang, P., et al., 2018. Influence of reflux ratio on two-stage anoxic/oxic with MBR for leachate treatment: performance and microbial community structure. Bioresour. Technol. 256, 69–76.
Lu, Z., He, Z., Parisi, V.A., et al., 2012. GeoChip-based analysis of microbial functional gene diversity in a landfill leachate-contaminated aquifer. Environ. Sci. Technol. 46 (11), 5824–5833.
Ma, B., Wang, H., Dsouza, M., et al., 2016. Geographic patterns of co-occurrence network topological features for soil microbiota at continental scale in eastern China. ISME J. 10 (8), 1891.
Ma, X., Vikram, A., Casson, L.W., et al., 2017. Centralized drinking water treatment operations shape bacterial and fungal community structure. Environ. Sci. Technol. 51, 7648–7657.
Peng, X., Guo, F., Ju, F., et al., 2014. Shifts in the microbial community, nitrifiers and denitrifiers in the biofilm in a full-scale rotating biological contactor. Environ. Sci. Technol. 48 (14), 8044–8052.
Saunders, A.M., Albertsen, M., Vollertsen, J., et al., 2016. The activated sludge ecosystem contains a core community of abundant organisms. ISME J. 10 (1), 11–20.
Shapiro, O.H., Kushmaro, A., Brenner, A., 2010. Bacteriophage predation regulates microbial abundance and diversity in a full-scale bioreactor treating industrial wastewater. ISME J. 4 (3), 327–336.
Shu, D., He, Y., Yue, H., et al., 2015. Microbial structures and community functions of anaerobic sludge in six full-scale wastewater treatment plants as revealed by 454 high-throughput pyrosequencing. Bioresour. Technol. 186, 163–172.
Singer, E., Wagner, M., Woyke, T., 2017. Capturing the genetic makeup of the active microbiome in situ. ISME J. 11, 1949–1963.
Sun, Y., Shen, Y.-X., Liang, P., et al., 2014. Linkages between microbial functional potential and wastewater constituents in large-scale membrane bioreactors for municipal wastewater treatment. Water Res. 56, 162–171.
van den Berg, E.M., van Dongen, U., Abbas, B., et al., 2015. Enrichment of DNRA bacteria in a continuous culture. ISME J. 9 (10), 2153–2163.
Vuono, D.C., Regnery, J., Li, D., et al., 2016. rRNA gene expression of abundant and rare activated-sludge microorganisms and growth rate induced micropollutant removal. Environ. Sci. Technol. 50 (12), 6299–6309.
Wang, X., Wen, X., Deng, Y., et al., 2016. Distance-decay relationship for biological wastewater treatment plants. Appl. Environ. Microbiol. 82 (16), 4860–4866.
Wang, H., Deng, N., Wu, D., et al., 2017. Long-term net transformation and quantitative molecular mechanisms of soil nitrogen during natural vegetation recovery of abandoned farmland on the Loess Plateau of China. Sci. Total Environ. 607, 152–159.
Wu, D., Huang, Z., Yang, K., et al., 2015. Relationships between antibiotics and antibiotic resistance gene levels in municipal solid waste leachates in Shanghai, China. Environ. Sci. Technol. 49 (7), 4122–4128.
Yan, Y., Kuramae, E.E., de Hollander, M., et al., 2017. Functional traits dominate the diversity-related selection of bacterial communities in the rhizosphere. ISME J. 11 (1), 56.
Ye, L., Zhang, T., 2013. Bacterial communities in different sections of a municipal wastewater treatment plant revealed by 16S rDNA 454 pyrosequencing. Appl. Microbiol. Biotechnol. 97 (6), 2681–2690.
Zhang, F., Peng, Y., Miao, L., et al., 2017. A novel simultaneous partial nitrification *Anammox* and denitrification (SNAD) with intermittent aeration for cost-effective nitrogen removal from mature landfill leachate. Chem. Eng. J. 313, 619–628.
Zhang, B., Zhang, J., Liu, Y., et al., 2018. Biogeography and ecological processes affecting root-associated bacterial communities in soybean fields across China. Sci. Total Environ. 627, 20–27.
Zhi, W., Yuan, L., Ji, G., et al., 2015. Enhanced long-term nitrogen removal and its quantitative molecular mechanism in tidal flow constructed wetlands. Environ. Sci. Technol. 49 (7), 4575–4583.